

Interaction Notes

Note 84

A NUMERICAL METHOD FOR OBTAINING THE CURRENT
AND CHARGE DISTRIBUTIONS, AND NEAR- AND
FAR-FIELDS OF THIN-WIRE STRUCTURES

July 1, 1971

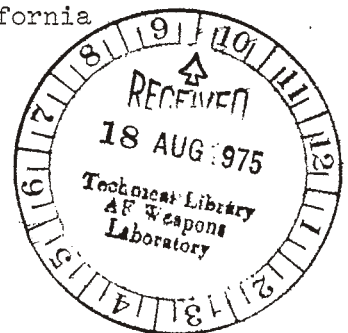
Sherman Gee^{*}, Edmund K. Miller^{**}, Andrew J. Poggio^{***},
Edward S. Selden, Gerald J. Burke
MBAssociates, P. O. Box 196, San Ramon, California 94583

Abstract

Computer techniques for solving electromagnetic radiation and scattering problems in the resonance region employing the thin-wire electric-field integral equation are discussed and demonstrated. The versatility and wide applicability of this approach for electromagnetic computer modeling are emphasized, and numerous sample results are presented to illustrate the method's accuracy and utility. Special attention is also devoted to evaluation of current and charge distributions on the structure and the near fields which result.

scattering, resonance, calculations, effects of EMP, magnetic fields,
electric fields, transmission

-
- * Now at Naval Ordnance Lab, Silver Springs, Maryland
** Now at Lawrence Livermore Laboratory, Livermore, California
*** Now at Cornell Aeronautical Lab, Buffalo, New York



I. Introduction

Tremendous strides have been made in recent years in adapting the rapidly growing computer technology toward solving electromagnetic problems of increased scope and complexity. Computer-aided solutions are now possible for many problems of practical interest which have resisted reduction to classically sought closed-form solution.

This paper is devoted to providing some insight into the power and value of computer techniques, and the diverse nature and scope of the electromagnetic problems toward which these methods are applicable. Since the computer revolution embraces nearly the entire electromagnetics spectrum, a subject much too broad to be examined in one paper, we shall restrict our attention to scattering and radiation analysis in the resonance region where analytical solutions are generally unavailable. Our attention will further be focussed on an area which has profoundly benefited from the digital computer, the integral equation formulation. Finally, our discussion will be devoted to one method or approach -- the thin-wire version of the electric-field integral equation.

This rather parochial viewpoint is taken so that the limited detail associated with broad coverage may be replaced by an indepth presentation which will convey the power and flexibility of such computer oriented methods. At the same time, the limitations of this kind of analysis can be more fully stated so as not to mislead the reader as to its capabilities. This presentation then is not so much a review paper as it is a concise picture of the important role of computer modeling in electromagnetics.

II. Theoretical Foundation

Since our primary concern here is the computer implementation of a numerical procedure and its typical applications rather than the accompanying theoretical preliminaries, we shall just outline the derivation of the integral equation used in the numerical modeling procedure. The formulation requires an integral relationship between the to-be-determined induced sources associated with an object and their resulting (secondary) fields. By evaluating the secondary field over a region where the total field behavior is known via boundary relations or continuity conditions, we are able to relate the unknown sources to the driving (primary) field which causes them. This leads to an integral equation for the unknown source distribution in terms of the specified primary field.

The starting point of our analysis is the thin-wire version of the electric field integral equation given by

$$\hat{s}(\bar{r}) \cdot \bar{E}^p(\bar{r}) = (i\omega\mu_0/4\pi) \int_{C(\bar{r})} I(s') \left\{ \hat{s}(\bar{r}) \cdot \hat{s}(\bar{r}') + \frac{1}{k^2} \frac{\partial^2}{\partial s \partial s'} g(\bar{r}, \bar{r}') \right\} ds' \quad (1)$$

where $\hat{s}(\bar{r})$ is a unit tangent vector at \bar{r} , \bar{E}^p is the primary field, I is the current, $C(\bar{r})$ is the structure geometry and is here used to imply an integration over all structures wires, $k = \omega\sqrt{\mu_0\epsilon_0}$ is the wave number with an assumed $\exp(i\omega t)$ time variation, and s' is a length variable along $C(\bar{r})$. The function $g(\bar{r}, \bar{r}')$ is the free space Greens function ($\exp(-ik|\bar{r}-\bar{r}'|)/|\bar{r}-\bar{r}'|$) specialized to the thin wire geometry; i.e., the observation point \bar{r} is assumed to be on the wire surface and the source point \bar{r}' on the wire axis (see Figure 1). In this way, the singularity in $g(\bar{r}, \bar{r}')$ is never encountered.

This particular thin-wire integral equation has been chosen for the analysis of wire structures because: 1) it is easily applicable to general geometries (or $C(\bar{r})$), 2) it maintains accuracy for small wire radius/wavelength values, and 3) the required current integration is analytically possible for certain types of current variation. Note that \bar{E}^p is arbitrary and may be due to an incident plane wave (in which case the structure's scattering characteristics are obtained) or due to localized excitation (from which the radiation properties of the structure as an antenna are derived).

An approximate solution for $I(s')$ in (1) can be obtained by reducing the integral equation to an N^{th} order system of linear equations in which the N unknowns are sampled values of the structure currents. The N equations are generated by enforcing the integral equation at N points (wire segments) on the structure (N values of \bar{r}). The coefficients in these equations are interpretable as mutual impedances and are dependent on structure geometry (see Appendix A). While there are many methods for accomplishing this reduction of the integral equation to a linear system (representable in matrix form), they differ only in detail and the computational effort required to obtain the matrix elements. Common to all such methods are the representation of the current in terms of its sampled values; a matching of the integral equation over the structure in some prescribed fashion; the numerical calculation of the N^2 "mutual impedance" coefficients; and subsequent solution of the linear system via inversion, factorization or iteration. A method for the expansion of the current in terms of sampled values is presented in Appendix B.

It may be appreciated that the process of generating a linear system to replace the integral equation is essentially one of evaluating the tangential electric field at point \bar{r} on the structure due to the current on a segment around \bar{r}' , with \bar{r} and \bar{r}' scanned over the structure geometry $C(\bar{r})$. The successful numerical modeling of a structure requires its representation by a collection of straight wire segments which is electromagnetically indistinguishable, within some specified accuracy criteria, from the original structure. Thus not only structures consisting entirely of straight wires, but curved wire structures, and solid surface objects as well, or combinations of these, are amenable to modeling in this fashion.

If the linear system representing the integral equation is written in matrix form as

$$[Z] [I] = [E] \quad (2a)$$

and the admittance matrix is found $[Y] = [Z]^{-1}$, it is a simple matter to evaluate the current distribution on the structure for any primary field through the matrix operation (See Appendix C for further discussion).

$$[I] = [Y] [E] \quad (2b)$$

All other electromagnetic field quantities such as near and far fields, polarization, impedance, etc. can then be found through other far less demanding operations. These processes are entirely consistent with Maxwell's equations and except for the integral equation solution method do not involve any a priori, and possibly, restrictive assumptions.

The procedure outlined above is of course not unique; every scattering and antenna problem involves a similar series of operations for its solution. Nor are the special features of the wire modeling approach new; the topic has been rather extensively documented (Richmond, 1966; Tanner and Andreasen, 1967). The main contribution of this presentation is to outline the method's computer implementation and to provide a convincing demonstration of its scope of applicability as evidenced by a variety of practical problems for which the technique has been profitably employed. The development of a dependable computer method is a process which requires an awareness of potential numerical limitations and a continued willingness to subject the computed results to experimental comparison as the scope of application is expanded. The numerical results included here are a representative cross-section of test cases of practical interest. The extensive validation to which the numerical procedure has been subjected allows its confident use as a computer-experimental tool.

III. Computer implementation

Development of a computer program based on the integral equation method is relatively straightforward. The difficulties in efficiently using the approach come from the many options open to the user pertaining to the desired output data (near or far fields; polarizations; bistatic or monostatic patterns; etc.) and the preparation of input data for the specific geometry of interest.

Prior to the generation of input data a suitable wire model to represent the structure must be developed. Modeling guidelines have evolved in the course of using the technique; a discussion of the numerical convergence with decreasing segment length for wire scatterers is presented elsewhere (Miller, et al., 1971). The wire structure geometry is then defined for the computer model in terms of the segment endpoints in cartesian coordinates, wire radius, and load impedance if any, for each

of the N structure segments, which are numbered $1, \dots, N$ for identification. Segment electrical connection information, required for the current interpolation procedure (see Appendix B), is supplied by two N -integer connection arrays, one of which pertains to the positive end of each of the segments relative to its current reference direction, and the other to the negative end. Positive integers, for example, are used for two segment junctions and denote the actual segment number to which the given segment is connected. Negative integers are used to denote connection of the segment to two or more other segments, identifiable by the same negative integer.

For structures such as the wire grid helicopter (see Figure 9), the data is generally derived segment-by-segment from scale drawings of the structure. This is an obvious area where future improvements could increase the effectiveness of computer modeling. An interactive graphics approach whereby the structure geometry data is automatically developed by the computer is possibly the most likely method of overcoming this problem. Many structures however consist largely of straight and/or curved wires or other systematically varying shapes which can be described by parametric equations so that subroutines can be used to generate these portions of the structure geometry. As a check on the geometry data for a new structure, a computer-drawn plot of the data can be generated and/or the data can be checked by a subroutine which verifies the compatibility of the connection and coordinate data with the program conventions (e.g. to verify that the electrical connections are physically correct). It is thus possible to eliminate virtually all errors in the geometry generator before proceeding with the actual calculation.

Having thus prescribed the structure being modeled, the subsequent steps in its numerical solution are the calculation of the impedance matrix, the matrix solution, the computation of the current, and finally the desired field evaluation. All of these operations (besides the initial integrations required for the impedance matrix evaluation) involve matrix manipulations. The storage and computer time required for them can be substantially reduced by structure symmetries which lead to a reduction in: 1) impedance matrix calculation time $\sim N^2/s$; 2) linear system solution time $\sim N^3/s^2$; and 3) current and field evaluation $\sim (N/s)$, where s is the number of symmetric sections which comprise the structure.

It is possible to effect additional solution efficiencies by specializing a computer program to a certain type or class of structures or by judiciously employing physically acceptable approximations in the solution procedure. A choice is frequently required between reducing solution cost for specific problems and developing a program of broad applicability. Generally speaking, it is desirable to have available a general purpose program which is adaptable with a minimum of change to particular problem applications.

The modeling capability of the integral equation (1) can be extended to problems other than conducting structures in free space by suitably modifying the Green's function for the problem of interest. The simplest extension is to a lossy medium, accomplished by using a complex wave-number in the integral equation. A more complicated problem is that of an antenna

near an interface of two semi-infinite media of different electrical properties, in which case a Green's function which involves the Sommerfeld integral can be used (Sommerfeld, 1964). Furthermore, the time-dependent equivalent of (1), obtainable by Fourier transformation can be used for transient studies. Examples from all of these extensions are shown below.

In concluding this section, we wish to emphasize that numerical methods both complement and supplement experimental measurement and classical theoretical analysis. It is not true to claim that the demonstration of a computer technique's validity for a limited range of problems proves it capable of solving any problem to which the technique might be applied. There are as yet many areas of uncertainty associated with computer modeling, and many rather simple problems for which satisfactory programs have not yet been developed. Techniques like that discussed above, while even now satisfyingly versatile, require continued improvement and extension. Modeling capabilities of this kind, if judiciously employed, do provide the initial phase of what eventually will become true computer experimentation.

IV. Scope of Applicability

The numerical solution of the integral equation allows in-depth analysis of a wide variety of electromagnetic problems. Radiation and scattering problems including mutual coupling can be treated with almost equal facility. A highly complex structure such as a helicopter (c.f. next section) has been successfully modeled employing the wire-grid equivalence described earlier. The use of wire-grid modeling provides a great flexibility in the type of structures which can be analyzed since conducting surfaces and structural details such as corners and wire appendages can all be effectively represented using wire segments. An indication of the wide scope of applicability of the technique is provided in Figure 2, where representative structures are listed with the required computation times and costs (on a CDC-6600 computer and a usage charge of \$1000/hour).

Both antenna radiation and scattering calculations are depicted in the figure. The first structure shown is a zig-zag dipole with a total wire length of 0.7λ . The input impedance at six different frequencies was determined for the computation time and cost indicated. The second structure is a fore-shortened log-periodic antenna where the four longest dipole elements are inductively loaded, demonstrating the modeling of impedance loading. The third configuration represents an unbalanced conical spiral antenna with wide tape arms, one of which is terminated by a reactive load. The wide tape arms are modeled here using two thin wires which conform to the edges of the tape. Additional cross wires can be placed on each arm to account for transverse currents if they prove significant. The fourth structure is the wire-grid equivalent of a parabolic reflector; the indicated computation time was required to calculate a single antenna pattern using a dipole feed. Distortions of localized regions of the reflecting surface and its effect on the electromagnetic characteristics can be easily

analyzed by appropriately modifying the geometric data. The fifth structure is a wire-grid representation of a slotted conducting plate for which the backscatter RCS of this structure at two frequencies, polarizations, and aspect angles were calculated. This suggests that the numerical approach is applicable to problems concerning electromagnetic coupling through surface apertures since the surface currents and aperture field distributions can be made available. The final structure is a "squirrel cage" which is a broadband scatterer for penetration-aid applications. The speed and accuracy with which the numerical computation are performed allow large scale parametric studies to be implemented which are highly suited to the iterative approach required in decoy design where the RCS of the scatterer is tailored to best match some desired (vehicle) RCS.

It is hoped that these examples provide an indication of the versatility of the numerical approach as applied to structures of various shapes and sizes. The next section presents additional examples in greater detail so that one can obtain an appreciation of the different type of solutions which are realizable.

VI. Typical Results

The usefulness of the integral equation technique considered above is best illustrated with sample results. Several types of applications are discussed in the following paragraphs.

The determination of possible corona discharge in the vicinity of an antenna requires a knowledge of the antenna near fields. Figure 3 is a plot of the normalized radial electric field of a loop antenna in the plane of the loop at an angle of 90 degrees from the source. Comparison with the published results of Fante, et-al. (1969) is shown. The near fields for a slightly more complicated configuration is shown in Figure 4. Two 9.3 inch diameter loops are each loaded with sixteen capacitive elements uniformly distributed along the conductor such that the loop resonates at 170 MHz. The upper loop is excited, and the lower loop, which is separated by 11 inches, acts as a parasitic element. The near fields (1 watt input power) are computed at a radial distance (from the z axis) equal to one inch plus the loop outer diameter. The fields are evaluated as a function of azimuthal angle ϕ from the z axis in the plane of the top loop (O), in the mid-plane (Δ), and in the plane of the bottom loop (x). The fields are respectively normalized to the three values (volts/meter) at the top of the figure. With this type of information one can predict where breakdown is most likely to occur and what, if any, techniques can be used to reduce this possibility.

Antenna input impedance can be calculated quite readily once the current on the antenna has been determined. For instance, Figure 5 shows the effect of the transmission line on the input admittance as a function of antenna electrical length and a comparison with results obtained using an ideal voltage source in the antenna. A complicated structure such as a Loran C antenna presents a more challenging problem. Computations have been performed to evaluate the input impedance of that antenna, over a

perfectly conducting ground, with the antenna excited near the base of the 625 foot mast. The twenty-four radial arms of catenary shape are joined at the top of the antenna. Figure 6 shows a comparison between the computed impedance and experimental data (supplied by the U.S. Coast Guard). Data such as this is useful in the design stage, and allows the performance of numerical "experiments" to determine the characteristics of various antenna configurations.

The calculation of radiation and scattering patterns is straightforward once the admittance matrix, Y , for a given structure has been obtained. Upon determining the current induced by the primary source (via multiplication of Y times the primary field vector), the secondary fields are obtained as an integration (analytic for the far field) of the structure currents. A bistatic pattern requires only one current evaluation, whereas the monostatic variation necessitates finding the current for each viewing angle desired. Figure 7 shows the backscatter radar cross section of a straight wire with bow-tie termination. Only data for $0 < \theta < 90$ degrees is shown because of the structure symmetry. The predictions are very accurate even in the region of the deep null.

Figure 8 illustrates the backscatter RCS as a function of aspect angle for the wire tee-pee shown, where a is the wire radius. The numerical data are plotted and compared with experimental data obtained by Micronetics, Inc. Two sets of experimental data are shown in Figure 8, representing clockwise and counterclockwise rotation of the angle θ .

Airborne platforms are generally complicated structures and accurate modeling, particularly in the resonance region, is required to accurately predict their electromagnetic characteristics. Wire grid models sufficiently represent solid surfaces when the open regions are small in terms of wavelengths (Richmond, 1966). Figure 9 shows numerical results obtained from a wire-grid model of an OH-6A helicopter compared with experimental data obtained by Collins Radio.

The interaction of an antenna and its environment can be quite pronounced when the environment is in the form of a ground plane. Although it is quite simple to predict antenna characteristics in the presence of a perfectly conducting ground plane, this simplicity is not realized when ground losses must be taken into account. The classical technique for handling the lossy ground problem is contained in the Sommerfeld integrals (Sommerfeld, 1964) which become part of the integral equation kernel. However, for antennas with any degree of complexity, the integrals can not be analytically evaluated and numerical integration is difficult and inefficient. An alternate, approximate technique, based on the Fresnel reflection coefficients, has been developed and has been shown to yield reliable results (Burke, et al., 1970). Figure 10 compares results using both methods as applied to a two element parasitic array of vertical antennas. The outstanding feature of the results presented is that the approximate technique reduced computation time by about two orders of magnitude compared to the time required employing the Sommerfeld formulation, with no significant loss of accuracy.

The transient (time domain) analysis of antennas and scatterers is another area of interest where the digital computer provides a unique capability. Using a Gaussian pulse for the exciting field, the time dependent currents induced on a structure can be evaluated by solving an integral equation which is the Fourier transform of Equation (1). Techniques for solving this type of equation are well known (Sayre, 1969); Bennett and Weeks, 1968; Poggio and Miller, 1970). It is a simple matter to evaluate the impulse response in the frequency domain from this information. In effect, the transfer function for the electromagnetic device is determined which can then be used to evaluate characteristics for other exciting waveforms. The advantage of the time domain analysis is that the frequency domain characteristics over a broad bandwidth can be determined with one relatively simple calculation.

Figure 11a shows the feed point current variation as a function of time for a dipole antenna excited with a Gaussian pulse at the center of the antenna. When the Fourier transform of this current is divided by the Fourier transform of the Gaussian pulse input voltage, the frequency domain input admittance is obtained as shown in Figure 11b. The results are compared with independent data as provided by King and Middleton (King, 1956). The bandwidth limitation and accuracy of the results are affected by time sample size, space sample size, the length of time over which the current is evaluated, and the subsequent accuracy with which this sampled data is transformed.

An example of a scattering application is shown in Figure 12. The problem of determining the time domain back scattered fields (or equivalently, the frequency domain RCS) from a crown band for axial incidence interest is presented in this figure. The time dependent response to a Gaussian pulse is presented in a) while the Fourier transform is used to determine the frequency domain response in b) over a finite bandwidth. Again, a comparison with independently computed results shows good agreement.

VII. Conclusions

The results shown above serve to illustrate the potential usefulness of the thin-wire, electric-field, integral equation for the numerical analysis of a variety of scattering and antenna problems. This approach, when combined with an efficient numerical method for its solution together with the speed and size of current digital computers, provides an economical and reliable alternative to, and complement for, the experimental study of a wide range of practical problems. These problems can include both thin-wire structures and wire grid models of solid-surface objects. Particular advantages are offered by the numerical method to determine such properties as average RCS, current-distributions, input impedance, near field behavior, etc., which may be difficult and expensive to measure experimentally.

APPENDIX A

NUMERICAL PROCEDURE

An outline of the numerical solution procedure for the induced current via reduction of the integral equation to a linear system is presented here.

The current integration in Equation (1) extends over the entire structure and produces the tangential electric field at any point on the surface. In mathematical terms, the current or source points lie in the domain, and the field or observation points in the range of the integral operator. An intuitive approach to solving the current is provided by: (1) approximating the current in terms of unknown sampled values and a specified functional variation on the structure; and (2) enforcing the resulting integrals to match the integral equation in a pointwise sense over the range of the integral operator. This procedure generates a set of linear equations for the unknown sampled current values and demonstrates at its simplest, the essence of the method of moments. Our discussion will be limited here to sub-sectional collocation, a version of the moment method, which is discussed in more general terms by Harrington (1969) and Kantorovich and Krylov (1964).

Let the actual structure current be approximated by

$$I(s') \approx \sum_{n=1}^N a_n f_n(s') \quad (A1)$$

where the a_n are constants to be determined and the f_n are the basis or trial functions. The f_n may be defined over the entire domain of the integral, or over a sequence of sub-domains. It is the latter approach which is used in the sinusoidal current expansion employed for the foregoing calculations. Upon substitution of (A1) into the integral equation (1), and requiring exact equality between the right and left hand sides of the equation at N points, p_m , $m = 1, \dots, N$ over the wire structure, we obtain, with $\partial/\partial s_m \equiv \hat{s}(p_m) \cdot \nabla$

$$\begin{aligned} & \frac{i\omega\mu_0}{4\pi} \sum_{n=1}^N a_n \int_C f_n(s') \left[\hat{s}(p_m) \cdot \hat{s}(s') + \right. \\ & \left. \frac{1}{k^2} \frac{\partial^2}{\partial s_m \partial s'} \right] g(p_m, s') ds' \quad (A2) \\ & = \hat{s}(p_m) \cdot \bar{E}^p(p_m) \\ & \quad m = 1, \dots, N \end{aligned}$$

which gives N equations for the N quantities a_n . This process of point-fitting the integral equation involves the use of delta functions for the weighting or testing functions employed in the approximation of the rigorous integral equation.

The linear system (A2) can be re-written in matrix form as

$$\sum_{n=1}^N Z_{mn} a_n = E_m$$

$$m = 1, 2, \dots, N$$

where Z and E are given by

$$Z_{mn} = \frac{i\omega\mu_0}{4\pi} \int_C f_n(s') \left[\hat{s}(p_m) \cdot \hat{s}(s') + \frac{1}{k^2} \frac{\partial^2}{\partial s_m \partial s'} \right] g(p_m, s') ds'$$

$$E_m = \hat{s}(p_m) \cdot \bar{E}^D(p_m)$$

Note that Z has the dimensions of impedance; hence its characterization as an impedance matrix. It represents the tangential electric field at point p_m on the structure due to the current term a_n . A solution for the a_n simply follows as

$$a_n = \sum_{m=1}^N Y_{nm} E_m \quad n = 1, \dots, N$$

where $Y = Z^{-1}$ is known as the admittance matrix. Since Y is derivable without dependence upon E , it truly approximates the electromagnetic response of the structure for which it has been obtained for any exciting primary field \bar{E}^D .

APPENDIX B

CURRENT INTERPOLATION

Let the current on segment j be expressed as

$$I_j(s') = A_j + B_j \sin k (s' - s_j) + C_j \cos k (s' - s_j) \quad (B1)$$

with s_j the midpoint coordinate (Yeh and Mei, 1967). Also, let segment j be connected to segments $j-1$ and $j+1$ at its minus and plus reference ends respectively with the reference directions on all three segments the same. Evaluation of I_j at s_{j-1} , s_j and s_{j+1} results in

$$\begin{aligned} A_j + C_j &= I_j \\ A_j - B_j s_{j-1,j} + C_j c_{j-1,j} &= I_{j-1} \\ A_j + B_j s_{j+1,j} + C_j c_{j+1,j} &= I_{j+1} \end{aligned} \quad (B2)$$

where d_j is the length of the j^{th} segment and

$$s \left| \begin{array}{l} \\ c \end{array} \right|_{j+1,j} = \begin{array}{l} \sin \\ \cos \end{array} \left[k (d_{j+1} + d_j)/2 \right]$$

Solution for A_j , B_j , and C_j in terms of I_{j-1} , I_j and I_{j+1} provides an equation of the form

$$I_j(s') = X_j(s') I_{j-1} + Y_j(s') I_j + Z_j(s') I_{j+1} \quad (B3)$$

where X_j , Y_j , Z_j contain the coefficients A_j , B_j , C_j . The system of equations which results from the collocation solution to the integral equation is thus seen to involve as unknowns the N current samples at the centers of the N segments into which the structure is divided.

The extension of the interpolation procedure to multiple junctions is straightforward. Consider the case where segment j is connected to m segments numbered $j+1, \dots, j+m$ at its plus end and the single segment $j-1$ at its minus end. Then only the equation representing (B1) evaluated at s_{j+1} is modified and becomes

$$A_j + \frac{1}{m} \sum_{i=j+1}^{j+m} B_j s_{i,j} + C_j c_{i,j} = \frac{1}{m} \sum_{i=j+1}^{j+m} I_i \quad (B4)$$

which comes from interpolating I_j to the midpoints of the m connected wires where it is equated to the average midpoint value. A solution for the A_j , B_j and C_j in terms of the midpoint currents I_{j-1} , I_{j+1} , ..., I_{j+m} follows as before. A multiple junction at the minus end of the segment is similarly treated.

Equation (B3) is substituted into the integral equation and, after summing over the N segments and collecting terms in I_j , gives

$$\frac{i\omega\mu_0}{4\pi} \sum_{j=1}^N I_j \left\{ \int_{d_{j+1}} X_{j+1} K_{j+1} ds' + \int_{d_j} Y_j K_j ds' + \int_{d_{j-1}} Z_{j-1} K_{j-1} ds' \right\} = \hat{s}(p_m) \cdot \bar{E}^P(p_m) \quad (B5)$$

with

$$K_j = \left[\hat{s}(p_m) \cdot \hat{s}(p_j) + \frac{1}{k^2} \frac{\partial^2}{\partial s_m \partial s_j} \right] g(p_m, s')$$

where by replacing $\hat{s}(s')$ by $\hat{s}(p_j)$ we implicitly assume that the individual wire segments are straight. The bracketed term in (B5) is interpretable as an impedance. It relates the current I_j , interpolated into neighboring segments, to the field at observation point p_m , $m = 1, \dots, N$.

APPENDIX C

NUMERICAL EVALUATION OF STRUCTURE CURRENT AND CHARGE DISTRIBUTION

The emphasis of the discussion in the main body of this presentation has been on the development and general application of the thin-wire computer modeling methodology to radiation and scattering problems. One aspect of this procedure which is of particular interest and relevance to the EMP area is that of determining the current and charge distributions on a structure exposed to some primary field of EMP origin. We, therefore, examine in greater detail here those features of the numerical treatment which bear most directly on the current and charge evaluation.

An essential feature of the numerical method is the approximation of the integral equation by a linear system whose solution can be achieved via standard matrix manipulations. Of particular import is the fact that the admittance matrix Y is the approximate numerical equivalent of the actual physical structure; its multiplication by a specified primary field vector leads to the induced structure currents in the numerical sense exactly as does illumination of the actual structure by the corresponding illuminating field in a physical sense. Furthermore, since knowledge of the structure current distribution allows straightforward computation of the resulting electromagnetic field anywhere in space, the admittance matrix can be regarded in a broad sense as a numerical hologram of the physical structure with the primary field vector serving as the reference beam used for reconstruction of the original wavefront. Actually, since from Y one can find the wavefront anywhere in space for any primary field, Y evidently contains much more information than the usual hologram, although it must be noted that an additional computation step is involved between the current calculation and the wavefront evaluation.

Continuing with the notation of Appendix A where the structure current is formally approximated by

$$I(s') \approx \sum_{n=1}^N a_n f_n(s') \quad (A1)$$

but adopting the specific sinusoidal current form given by (B1), we obtain explicitly for (A1)

$$I(s') \approx \sum_{n=1}^N [A_n + B_n \sin k(s' - s_n) + C_n \cos k(s' - s_n)] U(|s' - s_n|/d_n - 1)$$

$$\text{where } U(x) = \begin{cases} 1, & x \leq 0 \\ 0, & x > 0 \end{cases} \quad (C1)$$

Similarly, since the current $I(s')$ and charge density $\rho(s')$ are related via the continuity equation

$$\frac{\partial}{\partial s'} I(s') + \frac{\partial}{\partial t} \rho(s') = 0$$

we can express $\rho(s')$ as

$$\rho(s') \approx i \sqrt{\mu_0 \epsilon_0} \sum_{n=1}^N [B_n \cos k(s' - s_n) - C_n \sin k(s' - s_n)] U(|s' - s_n|/d_n - 1) \quad (C2)$$

Thus, a determination of the charge and current distribution on the structure first requires evaluation of the current expansion coefficients A_j , B_j , and C_j on the N structure segments.

From Appendix B, where the current interpolation is discussed, it is clear that the unknowns in the linear system (2a) are the sampled current values, I_j , at the centers of each of the N structure segments. Furthermore, the A_j , B_j and C_j on a given segment are expressible in terms of the sampled current values on that segment and the segments to which it is connected. It is thus possible to write (C1) and (C2) in terms of Y and the various interpolation functions $X_j(s')$, $Y_j(s')$ and $Z_j(s')$, $j=1, \dots, N$ [introduced in (B3)]. Since, however, the interpolation functions contain common $\cos k(s' - s_j)$ and $\sin k(s' - s_j)$ factors, it is computationally more efficient to use the forms for $I(s')$ and $\rho(s')$ given by (C1) and (C2) with prior numerical evaluation of A_j , B_j and C_j from the admittance matrix.

For the simply connected structure (no multiple wire junctions), we have

$$A_j = D_j^{-1} \left\{ [-s_{j-1,j} c_{j+1,j} - s_{j+1,j} c_{j-1,j}] I_j + s_{j+1,j} I_{j-1} + s_{j-1,j} I_{j+1} \right\}$$

$$B_j = D_j^{-1} \left\{ [c_{j-1,j} - c_{j+1,j}] I_j + [c_{j+1,j} - 1] I_{j-1} - [c_{j-1,j} - 1] I_{j+1} \right\}$$

$$C_j = D_j^{-1} \left\{ [s_{j-1,j} + s_{j+1,j}] I_j - s_{j+1,j} I_{j-1} - s_{j-1,j} I_{j+1} \right\}$$

$$\text{with } D_j^{-1} = s_{j+1,j} [1 - c_{j-1,j}] + s_{j-1,j} [1 - c_{j+1,j}]$$

Thus once the sampled current values have been calculated from

$$I_n = \sum_{m=1}^N Y_{nm} E_m \quad (C4)$$

with E_m the tangential component of the primary field at the center of the n 'th segment, numerical values for the current expansion coefficients can be computed from (C3) followed by application of (C1) and (C2) to obtain the charge and current distribution. The procedure is more involved but essentially the same for the situation posed by the multiple junction case where as a result (C3) would be modified as discussed in Appendix B.

Having obtained the current expansion coefficients, computation of other field variables is straightforward. While the far-field is perhaps the most commonly sought quantity for both radiation and scattering problems, the near-field is just as subject to evaluation. The principal difference in computing these fields is the analytic current integration that is possible in the calculation of the far-field whereas the near-field determination requires some numerical integration. In either case, the field due to the current induced on the structure is given by

$$\begin{aligned} \bar{E}(\bar{r}) = \frac{i\omega\mu_0}{4\pi} \sum_{n=1}^N \int_{-d_n/2}^{d_n/2} [A_n + B_n \sin k(s' - s_n) \\ + C_n \cos k(s' - s_n)] U(|s' - s_n|/d_n - 1) [\hat{s}_n + \frac{1}{k^2} \nabla \frac{\partial}{\partial s_n}] g_n(\bar{r}) ds' \end{aligned} \quad (C5)$$

where $g_n(\bar{r}) = \exp(-ik |\bar{r} - \bar{r}_n|) / |\bar{r} - \bar{r}_n|$

and $\bar{r}_n = \bar{r}_{n0} + s' \hat{s}_n$

with \bar{r}_{n0} the position vector to the center of segment n and $\hat{s}_n = \hat{s}(p_n)$.

ACKNOWLEDGMENT

The authors gratefully acknowledge the contributions of Drs. G. M. Pjerrou, A. R. Neureuther and Mr. H. L. Bosserman who were instrumental in the original development of the thin-wire computer program.

REFERENCES

- J. H. Richmond, IEEE Trans. Ant. Prop., AP-14, 782 (1966)
- R. L. Tanner and M. G. Andreason, IEEE Spectrum, 4, 53 (1967)
- E. K. Miller, G. J. Burke, and E. S. Selden, IEEE Trans. Ant. Prop., AP-19, to be published (1971)
- A. Sommerfeld, "Partial Differential Equations in Physics", Academic Press, New York (1964)
- R. L. Fante, J. J. Otazo, and J. T. Mayhan, Radio Science, 4, 697 (1969)
- E. K. Miller and B. J. Maxum, Final Report No. ECOM-0456-1, USAECOM, Ft. Monmouth, N. J. (1970)
- G. J. Burke, S. Gee, E. K. Miller, A. J. Poggio, and E. S. Selden, Proceedings 20th Annual Symposium on USAF Antenna R & D, Allerton Park, Monticello, Illinois (1970)
- E. P. Sayre, Technical Report TR-69-4, Syracuse University (1969)
- C. L. Bennett, Jr., and W. L. Weeks, Technical Report TR-EE68-11, Purdue University, Lafayette, Indiana (1968)
- A. J. Poggio and E. K. Miller, Tech Memo MB-TM-70/20, MBAssociates, San Ramon, California (1970)
- R. W. P. King, "The Theory of Linear Antennas", 149, Harvard University Press, Cambridge, Mass. (1956)
- R. F. Harrington, Proc. IEEE, 55, 136 (1967)
- L. V. Kantorovich and V. F. Krylov, "Approximate Methods of Higher Analysis", Interscience, New York (1964)
- Y. S. Yeh and K. K. Mei, IEEE Trans., AP-15, 634 (1967)

FIGURE CAPTIONS

Figure

- 1 Geometry for thin wire electric-field integral equation
- 2 Diversity of structures and cost comparisons
- 3 Loop antenna near fields
- 4 Near-field variation in the vicinity of a capacitively-loaded dual-loop antenna
- 5 Admittance versus kL including transmission line effect
(G is the conductance and B the susceptance)
- 6 Input impedance of Loran C antenna over perfectly conducting ground
- 7 RCS for straight-wire with bow-tie terminations
- 8 RCS for wire tee-pee
- 9 Radiation pattern for towel bar homing antenna on OH-6A helicopter
- 10 Input impedance and radiation patterns for an array of two half-wave dipoles over lossy ground
- 11 Dipole antenna excited by a Gaussian pulse
- 12 Scattering of a Gaussian pulse by a crown band

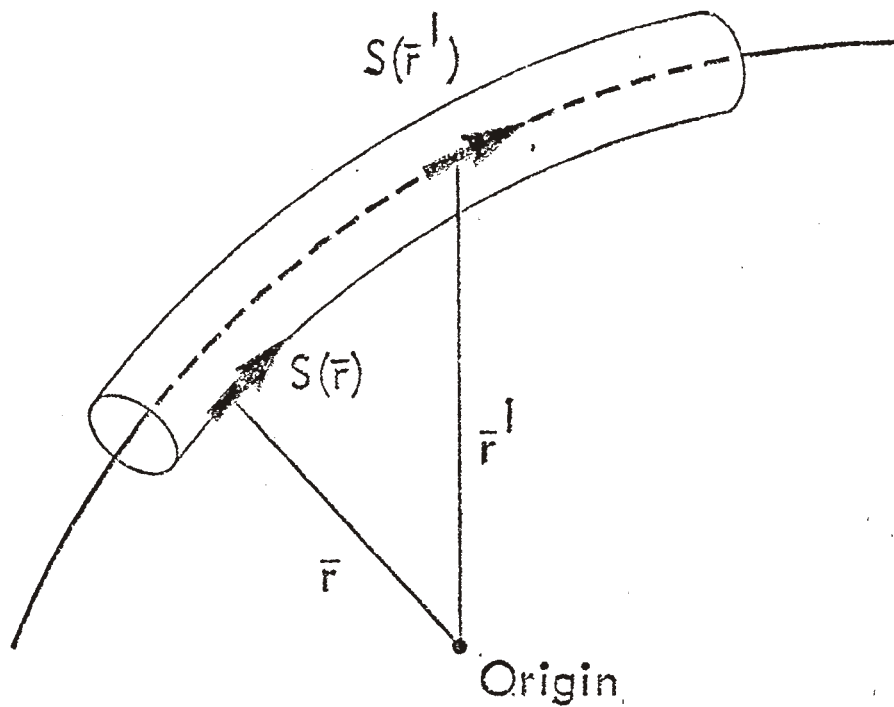


FIGURE 1.
GEOMETRY FOR THIN WIRE ELECTRIC
FIELD INTEGRAL EQUATION

No. Freqs (F)
Impedance Z

No. Patterns [P]

No. Angles (k)

Backscatter RCS $\sigma_n(\pi)$
n Polarization

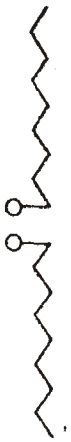
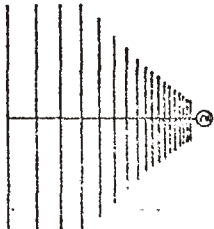
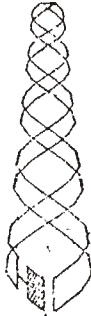
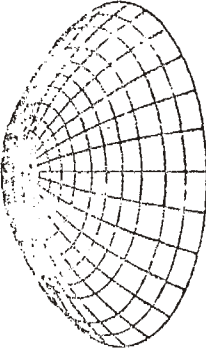
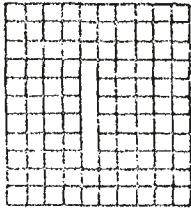
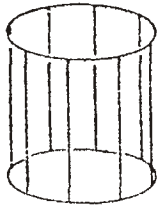
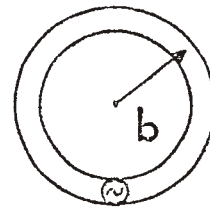
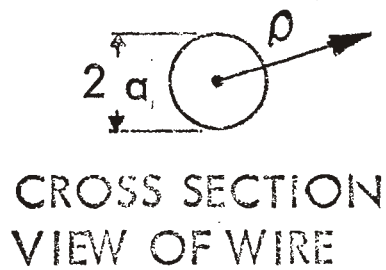
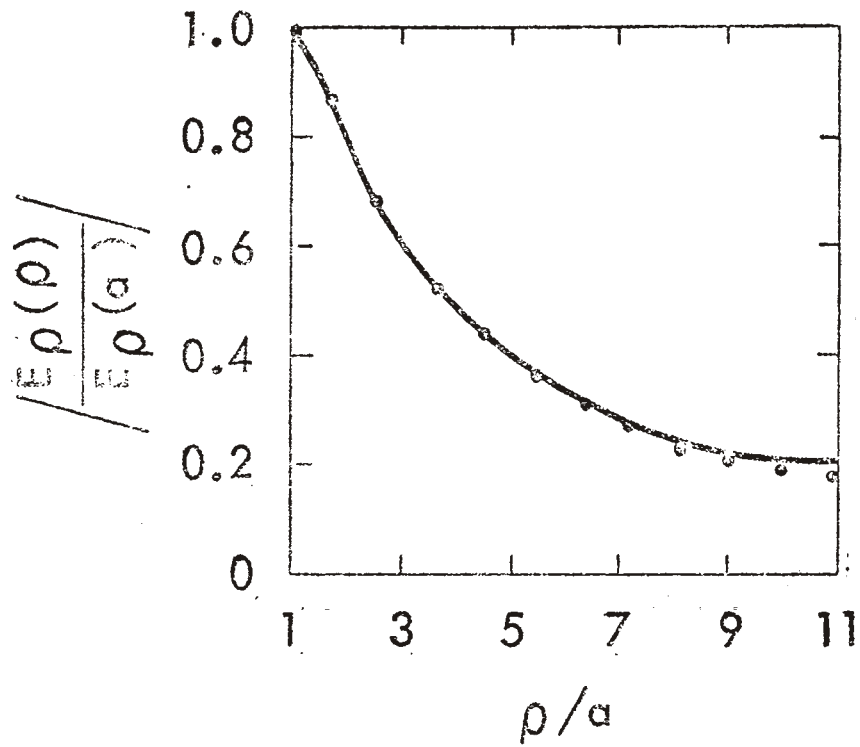
Structure						
Output Data	Z 6 (F) 0.7 λ	2[P(θ, ϕ)] 19.4 λ	4[P(θ, ϕ)] 3.8 λ	1[P(θ, ϕ)] 113.6 λ	$\sigma_2(\pi)$ 2(F,k) 12 λ	$\sigma_2(\pi)$ 23(k) 4.1 λ
CDC 6600 Time	39 Sec.	70 Sec.	68 Sec.	147 Sec.	77 Sec.	62 Sec.
Computation Cost	\$9	\$17	\$16	\$35	\$18	\$15

FIGURE 2. DIVERSITY OF STRUCTURES AND COST COMPARISONS



— PUBLISHED RESULTS (FANTE, et al., 1969)

• INTEGRAL EQUATION RESULTS

$$a/b = 3.5 \times 10^{-2}$$

$$kb = 1.0$$

$$\Phi = \pi/2$$

FIGURE 3.
LOOP ANTENNA NEAR FIELDS

Dual Loop (Sep. = 11)

$E_{max} = 447.113 \quad 63.230 \quad 22.657$

Freq MHz = 190.0

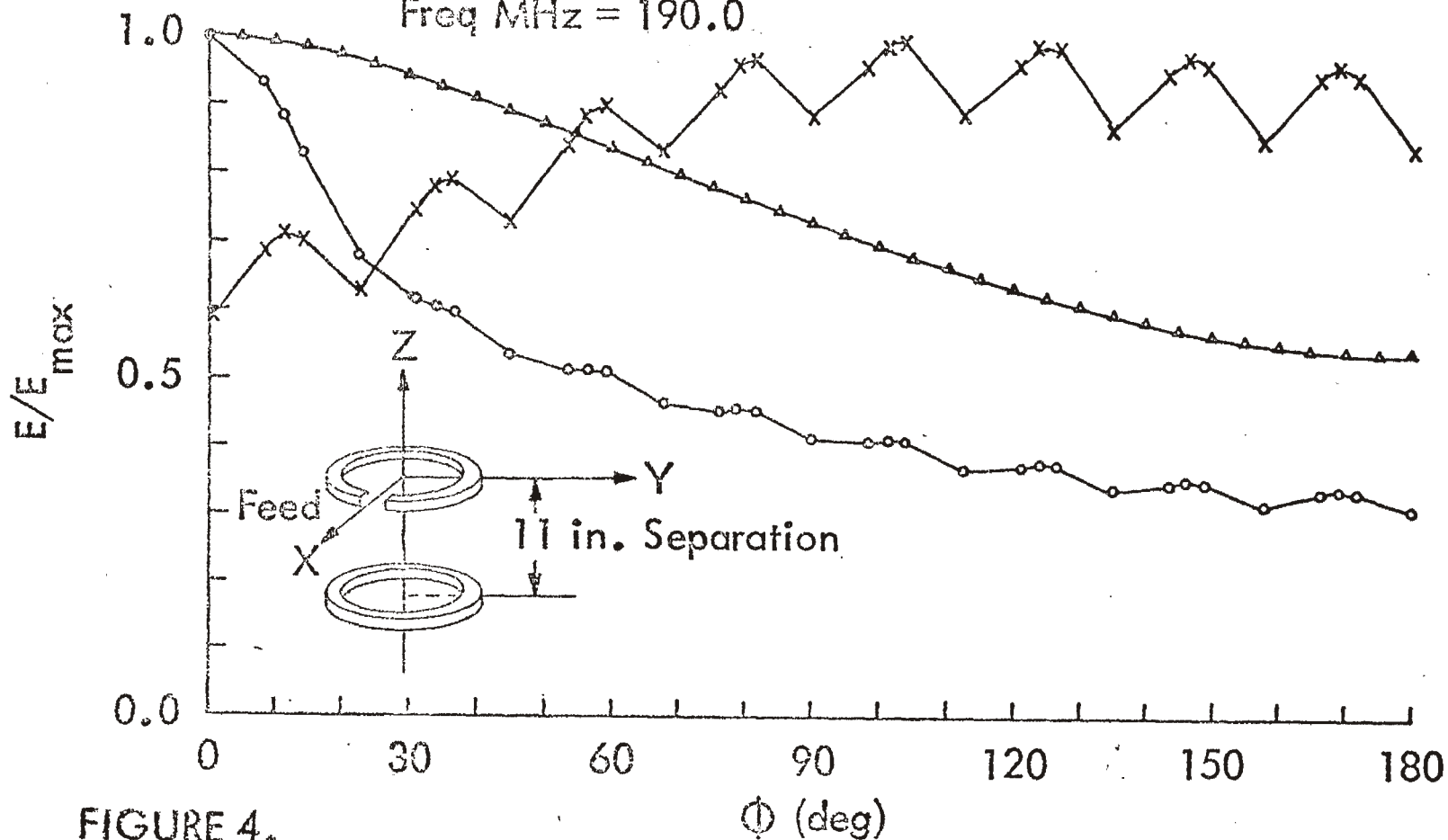


FIGURE 4.

NEAR FIELD VARIATION IN THE VICINITY OF A CAPACITIVELY-LOADED DUAL-LOOP ANTENNA

— Transmission-Line Source

- - - Simple Source

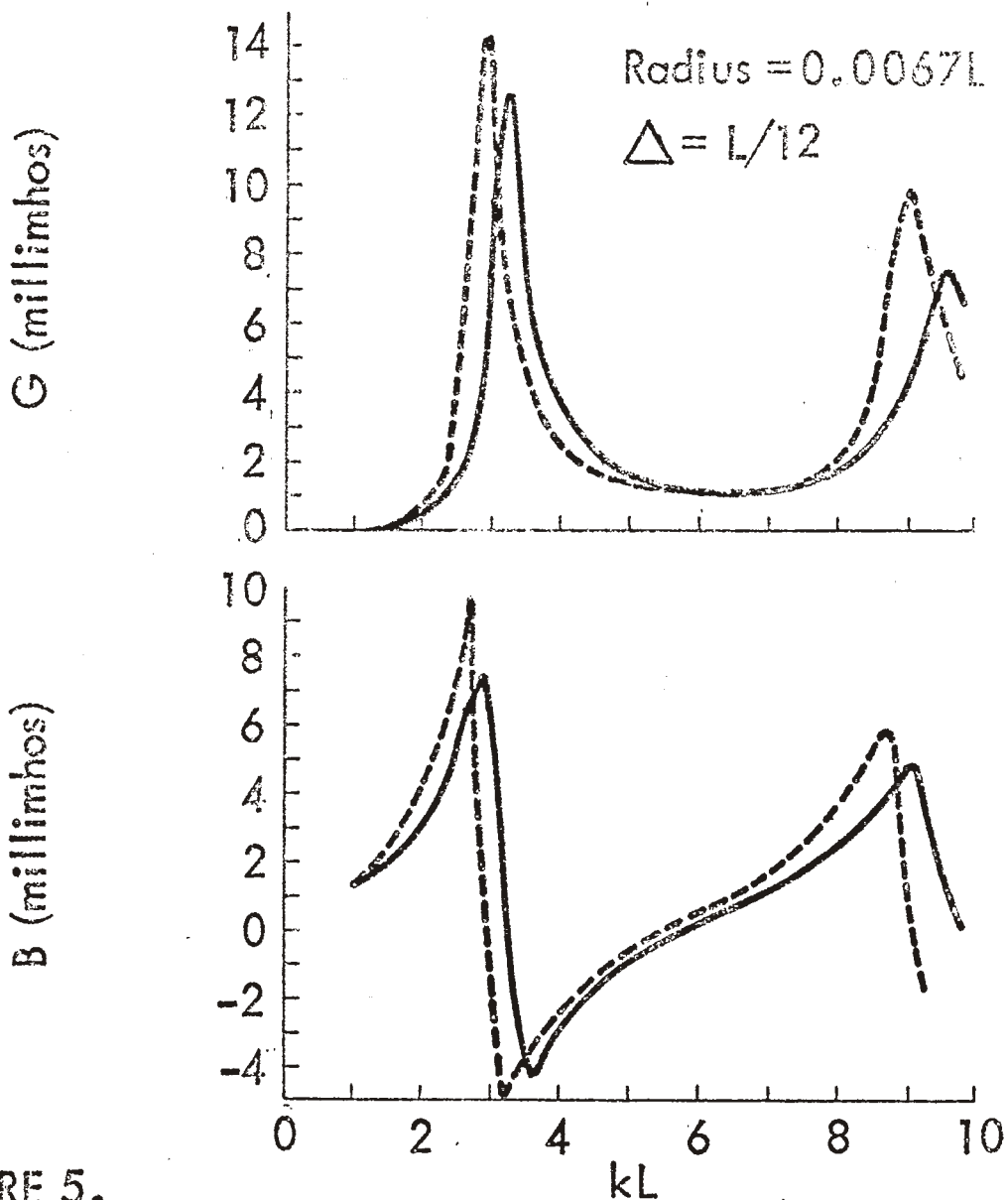
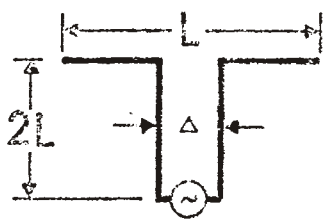


FIGURE 5.
 ADMITTANCE VERSUS kL INCLUDING TRANSMISSION
 LINE EFFECT (G IS THE CONDUCTANCE AND B THE
 SUSCEPTANCE)

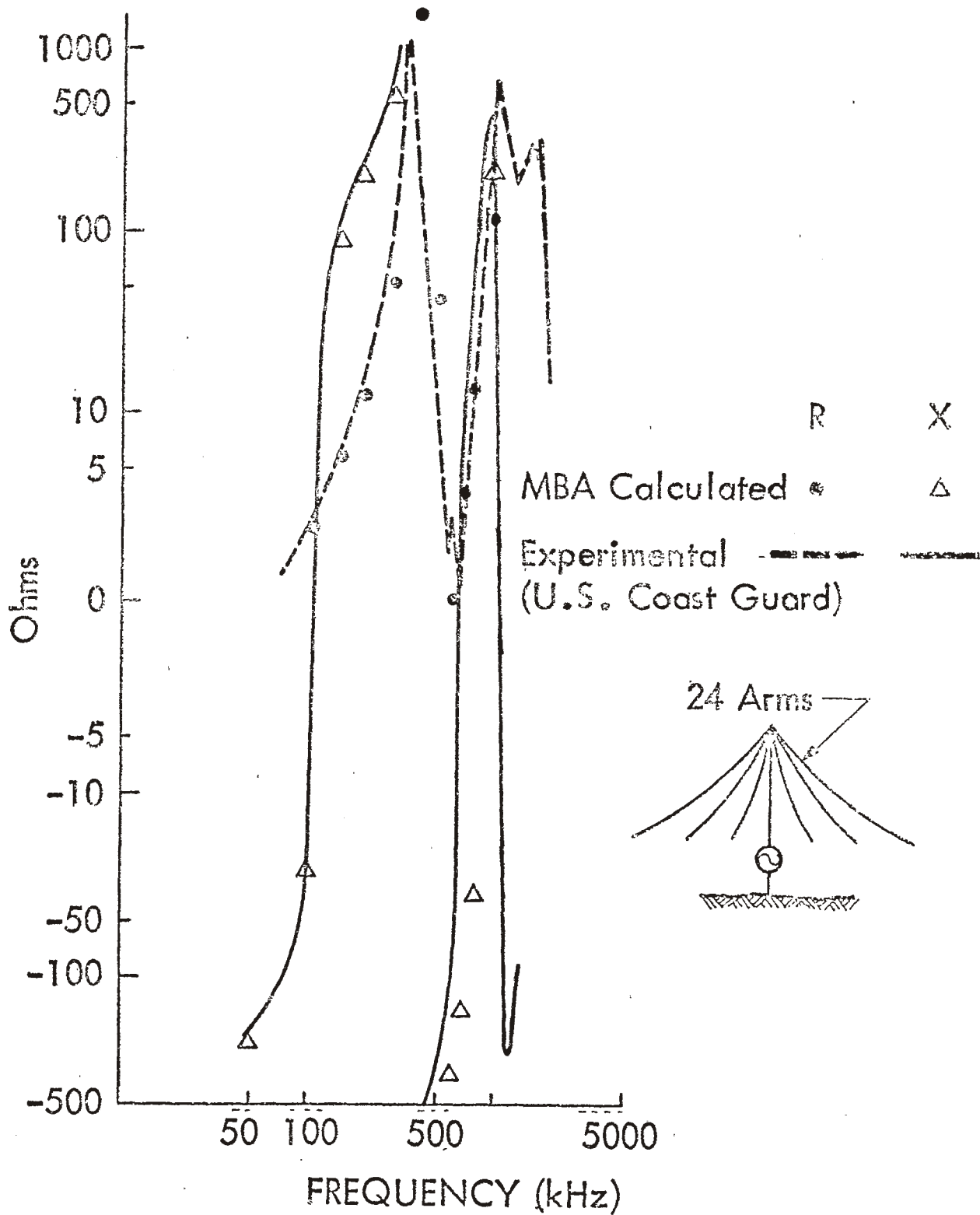
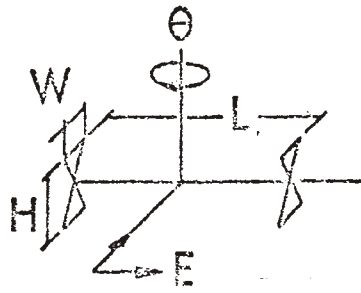


FIGURE 6.
 INPUT IMPEDANCE OF LORAN C ANTENNA
 OVER PERFECTLY CONDUCTING GROUND



$$a/\lambda = 0.0035$$

$$L/\lambda = 2.09$$

$$H/\lambda = 0.52$$

$$W/\lambda = 0.25$$

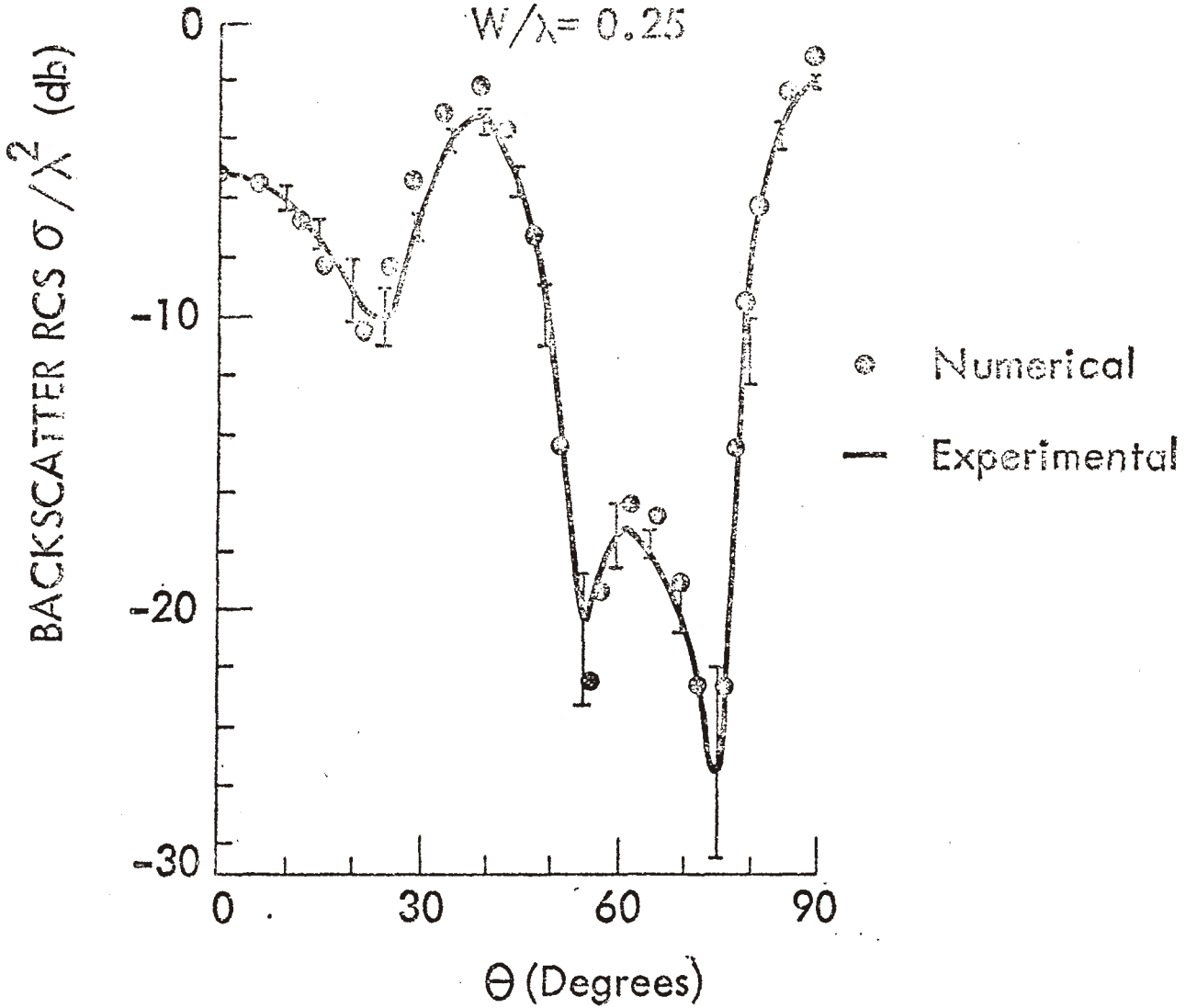
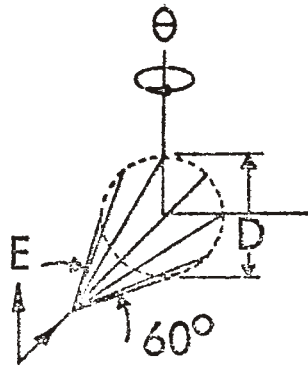


FIGURE 7.
RCS FOR STRAIGHT WIRE WITH BOW-TIE TERMINATIONS



$a/\lambda = 0.0035$
 $D/\lambda = 1.05$

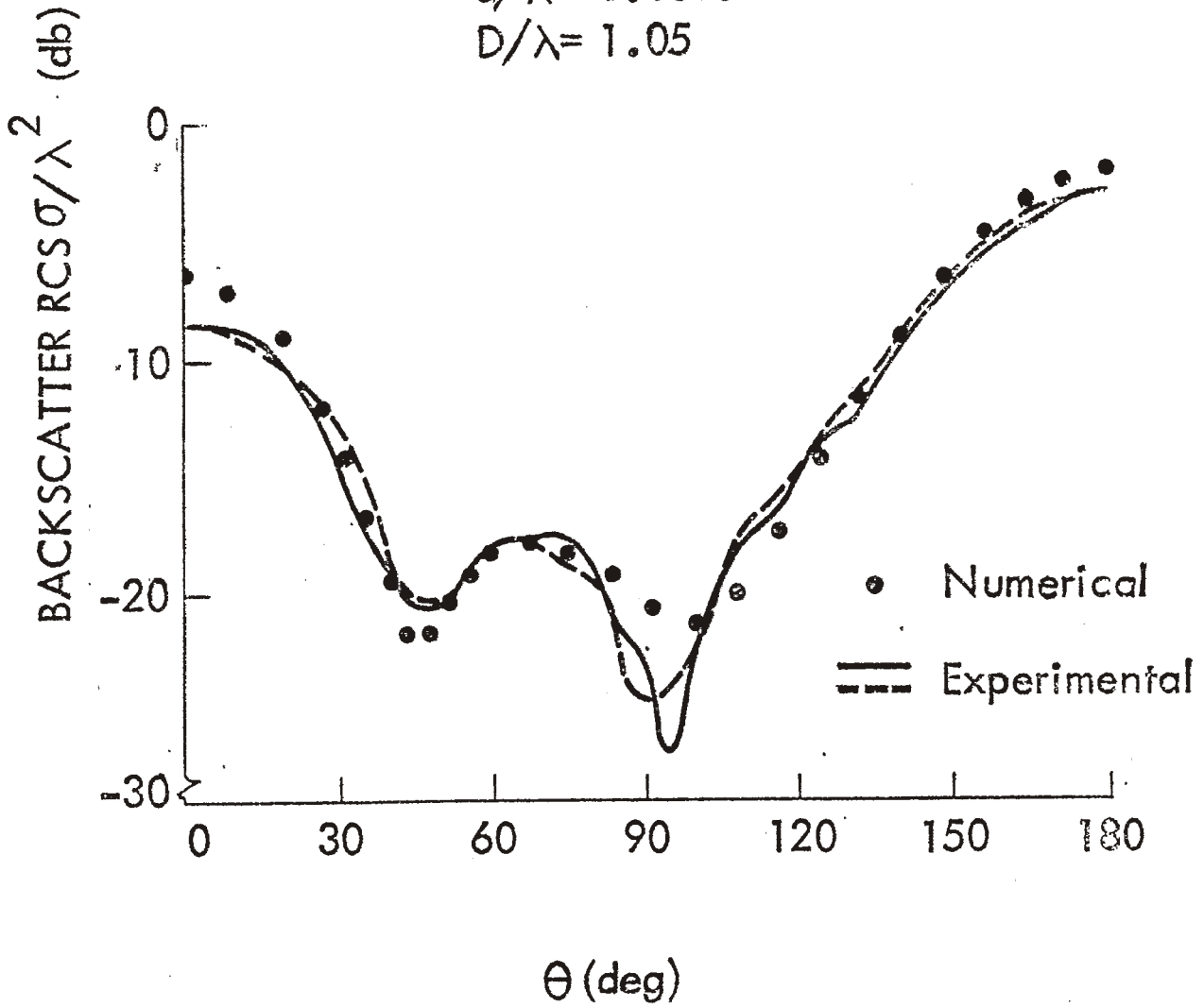


FIGURE 8.
RCS FOR WIRE TEE-PEE

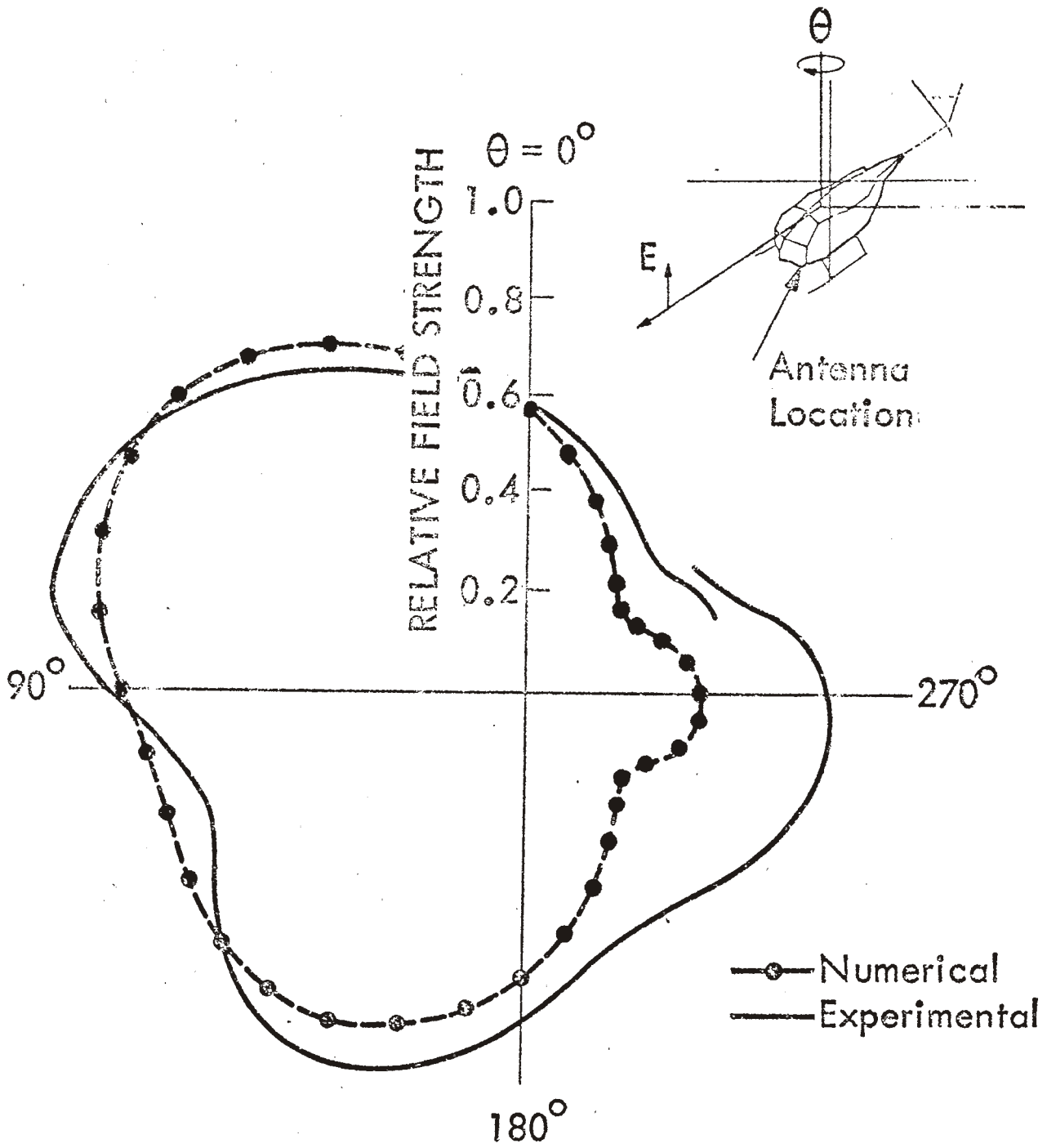
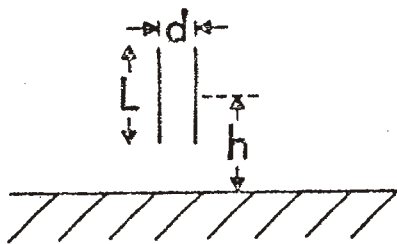
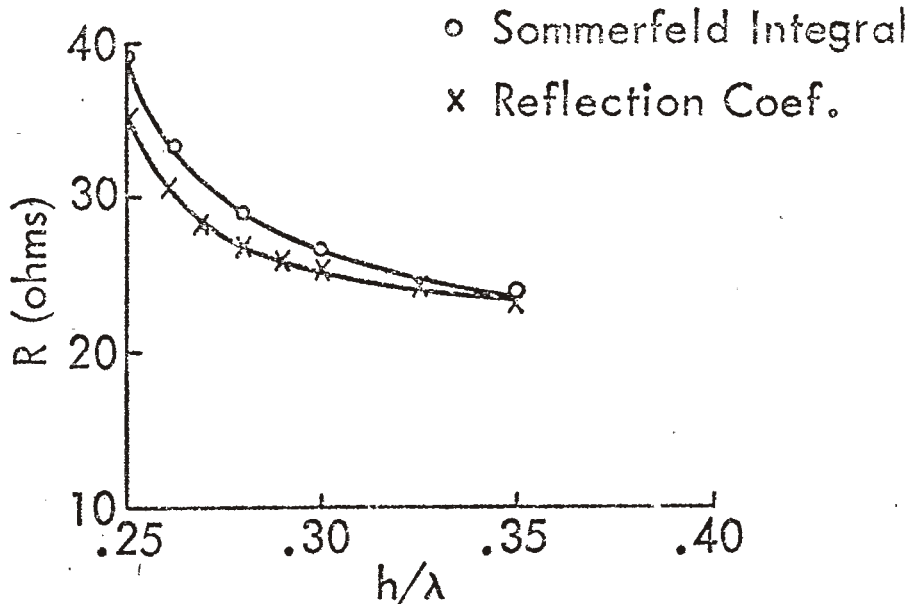


FIGURE 9.
 RADIATION PATTERN FOR TOWEL BAR HOMING
 ANTENNA ON OH-6A HELICOPTER

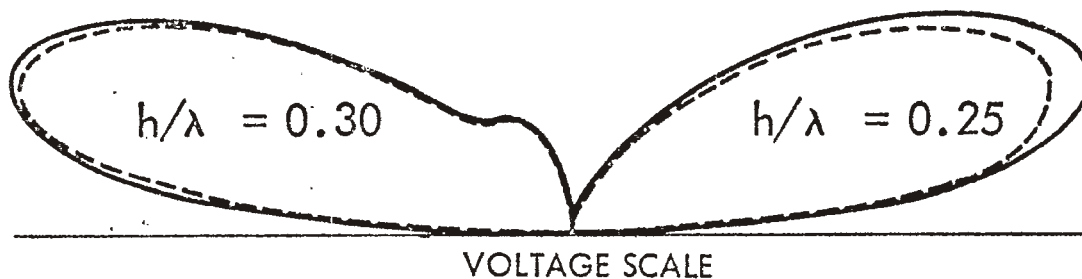


Separation $d = 0.1\lambda$
 Dipole Length $L = 0.5\lambda$
 $\epsilon_r = 10.0; \sigma = 3 \times 10^{-3}$
 Frequency = 3.0 MHz



a) Input Impedance

— Reflection Coefficient
 - - - Sommerfeld Integral



b) Radiation Patterns

FIGURE 10.
 INPUT IMPEDANCE AND RADIATION PATTERNS
 FOR AN ARRAY OF TWO HALF-WAVE DIPOLES
 OVER LOSSY GROUND

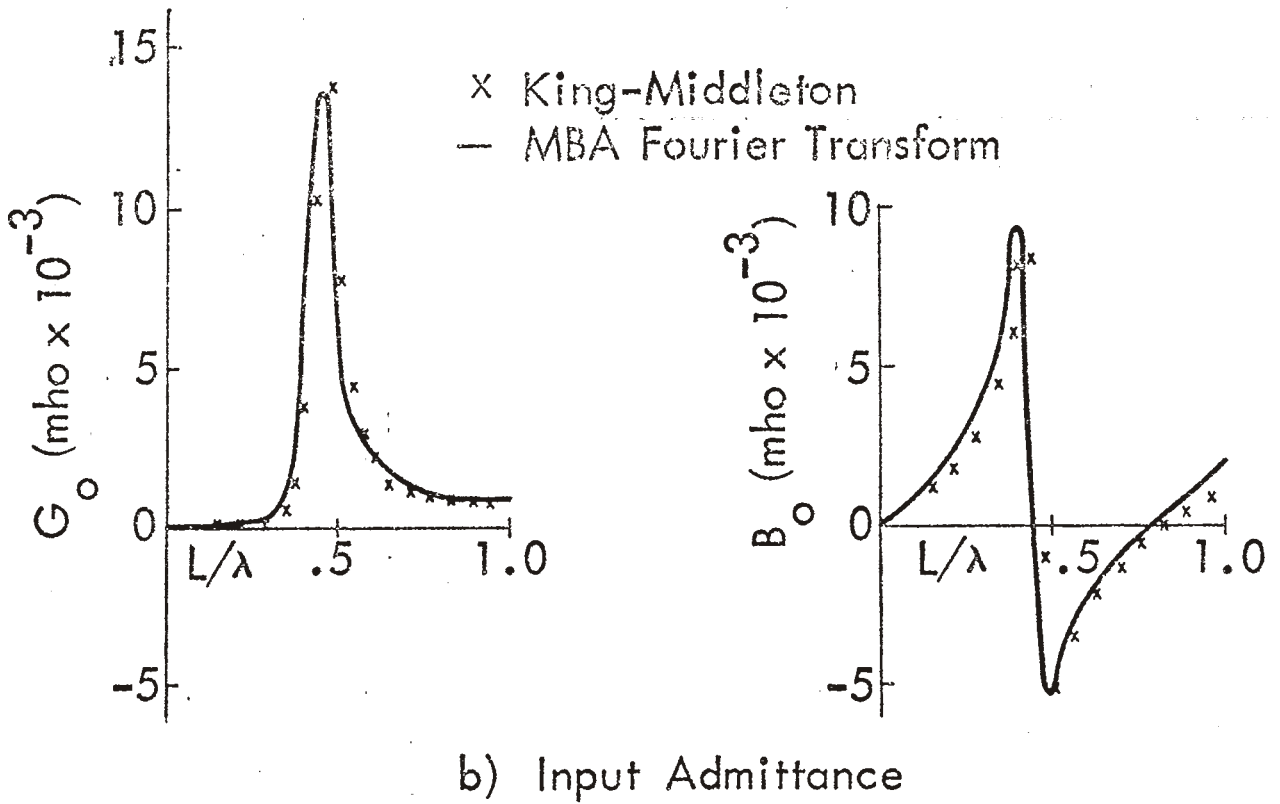
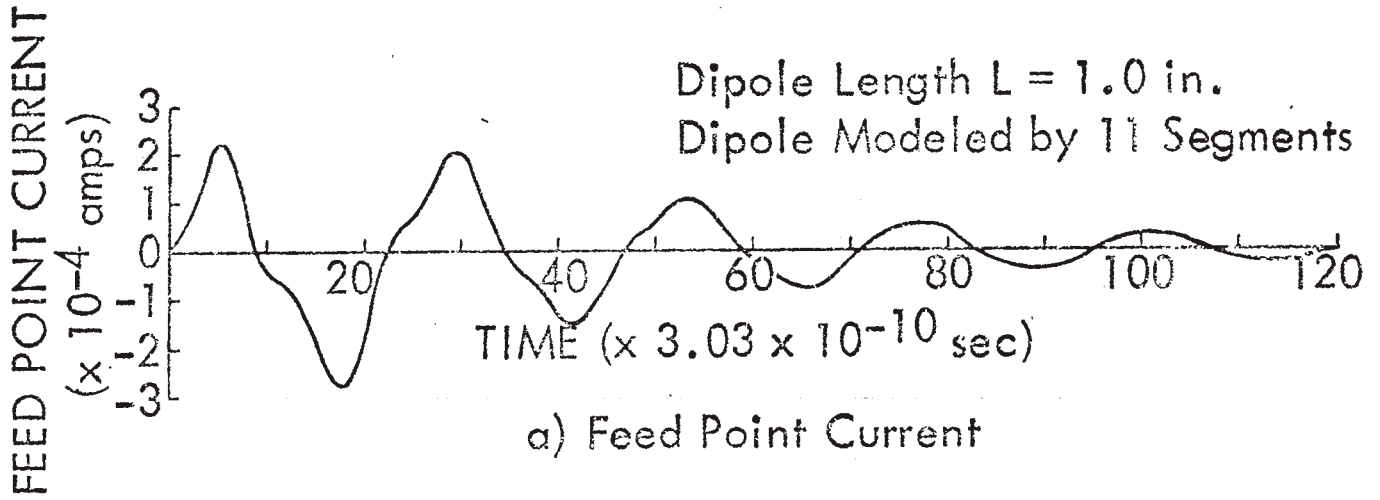


FIGURE 11.
DIPOLE ANTENNA EXCITED BY A GAUSSIAN PULSE



Circumference, $P = 25.13$ in.
 Wire Length = 84.0 in.
 Wire Radius = 0.0625 in.
 36 Segments

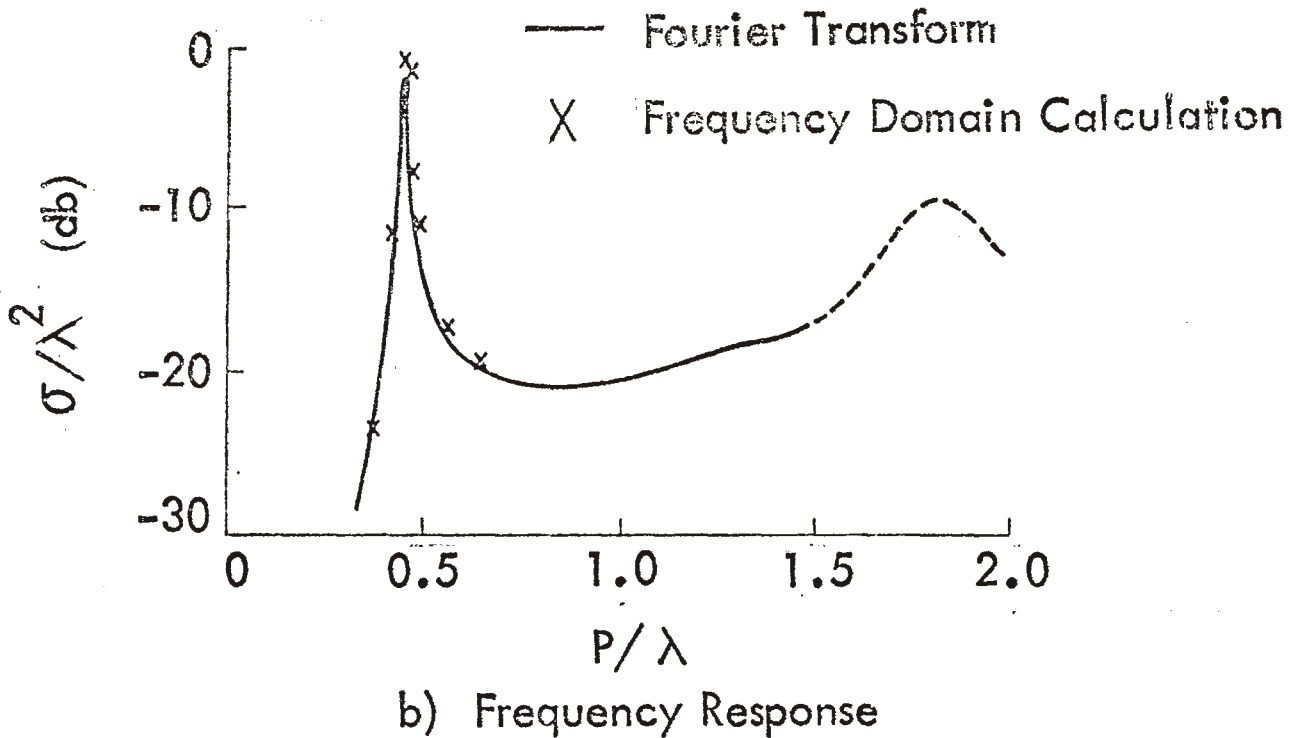
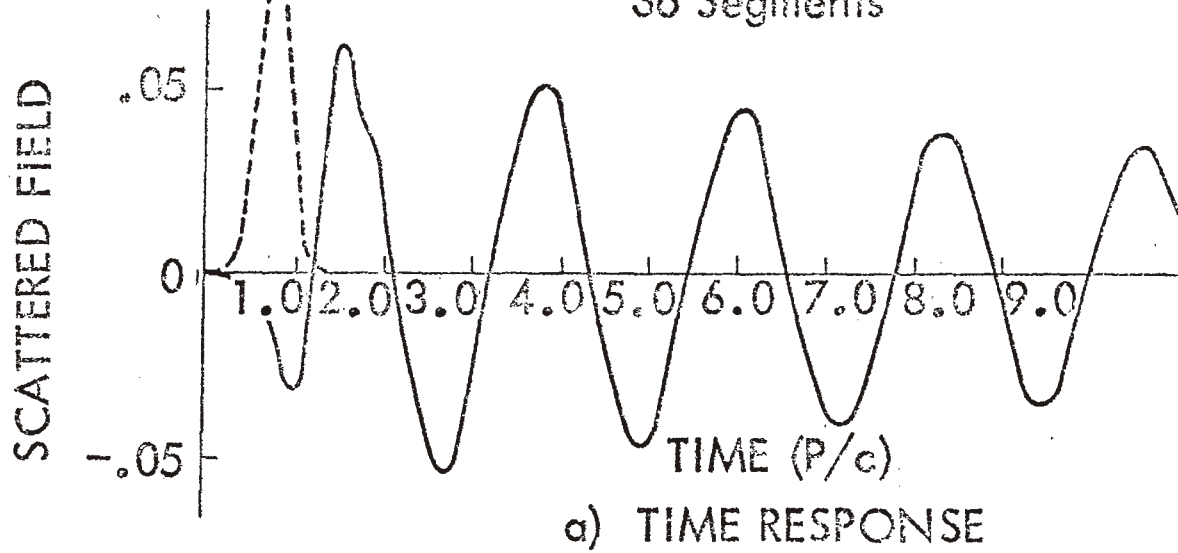


FIGURE 12.
 SCATTERING OF A GAUSSIAN PULSE BY A CROWN BAND